Validation of the MadAnalysis 5 implementation of ATLAS-SUSY-2013-21

Guillaume Chalons, Dipan Sengupta (LPSC Grenoble)

email: chalons@lpsc.in2p3.fr,sengupta@lpsc.in2p3.fr

August 26, 2015

Abstract

In this note we summarise the validation of the implementation in the `MadAnalysis5` framework of the ATLAS search targeting either the flavour violating decay of the lightest stop to a charm quark and a neutralino $\tilde{t}_1 \rightarrow c + \tilde{\chi}_1^0$, or compressed supersymmetric scenarios [1]. This search was performed by ATLAS using either a monojet or a charm-tagging selection. We only implemented the monojet analysis since we cannot emulate the charm-tagging.

1 Description of the implementation of the analysis

The analysis was implemented using the `MadAnalysis5 v1.1.11` (`MA5`) framework [2] with the `delphesMA5tune` detector simulation. To validate our analysis we compared our results with three official ATLAS cutflows (taken from [3]) obtained from three different benchmark points which we present below:

- **8TeV_t200_n125**: This benchmark point targets the $\tilde{t}_1 \rightarrow c + \tilde{\chi}_1^0$ simplified topology with BR($\tilde{t}_1 \rightarrow c + \tilde{\chi}_1^0$) = 100%. The stop mass is fixed at $m_{\tilde{t}_1} = 200$ GeV and $m_{\tilde{\chi}_1^0} = 125$ GeV.

- **8TeV_t200_n195**: This benchmark is the same as above but with $(m_{\tilde{t}_1}, m_{\tilde{\chi}_1^0}) = (200, 195)$ GeV.

- **8TeV_t250_n245**: Same as the first one with $(m_{\tilde{t}_1}, m_{\tilde{\chi}_1^0}) = (250, 245)$ GeV.

Two different analysis strategies were designed in [1] to optimise the sensitivity for direct stop pair production where stops decay into a charm quark and the lightest neutralino ($\tilde{t}_1 \rightarrow c + \tilde{\chi}_1^0$): a monojet and a charm-tagging (c-tagged) analyses. These analyses can also be used to investigate compressed supersymmetric (SUSY) spectrum. In this work we only implemented the monojet-like analysis since we cannot reproduce the c-tagging since it is not documented enough in [1]. To increase the sensitivity to small mass splittings between the stop and the neutralino the

1

monojet event selection relies on a hard initial-state-radiation (ISR) jet to identify signal events. The analyis is divided in three signal regions (SR) $M_{1,2,3}$ defined according to the p_T of the leading jet and the amount of missing transverse energy E_T^{miss}.

To validate the analysis we generated 10^5 at the parton level events for each of the above benchmark points using `MadGraph5_v1.4.8` (`MG5`) (with the PDF set`CTEQ6L1`) [4] (as used by the ATLAS collaboration to generate their own signal samples in [1]) and made use of `Pythia6.4.24` within the `pythia-pgs` package of `MG5`for showering and hadronisation. We use the `AUET2B` tune of `PYTHIA` to treat the underlying event [5]. The parameter cards in the form of `slha` files are provided by the `ATLAS` collaboration on `HEPDATA` [6]. We used our own cards for generating the events. The `QCUT` and `XQCUT` parameters needed for the merging are defined as $m_{\tilde{t}_1}/4$. The generated files in the `StdHep` format were then passed through detector simulation using the modified version of `DELPHES3` [7] as implemented in `MadAnalysis5`. The `DELPHES` card used is available at [8] which is the same as the one used for the validation of the ATLAS SUSY 13 05 analysis. Jets were reconstructed with an anti-k_t algorithm with a jet radius parameter $R = 0.4$, and we consider reconstructed jets with $p_T > 20$ GeV and $|\eta| < 2.8$. Electrons were required to satisfy $p_T > 20$ GeV and $|\eta| < 2.47$ and muons $p_T > 20$ and $|\eta| < 2.4$. The number of events was rescaled to a luminosity of $20.3\mathrm{fb}^{-1}$ using the tabulated 8 TeV stops/sbottoms production cross sections with squarks and gluinos decoupled [9].

2 Results and plots

We present in this section the `MA5` counterpart of the official figures provided in [1]. We first discuss the cutflows, then the histograms and finally the reproduction of the 95% CL limit setting figure in the $(m_{\tilde{t}_1}, m_{\tilde{\chi}_1^0})$ plane.

2.1 Cutflows

The ATLAS collaboration provided three cutflow tables for the three above mentionned benchmark points. The comparison between our reimplementation and the official ATLAS results are presented in Tables 1, 2, 3.

Before applying the cuts and after rescaling the number of events given by `MadGraph-Pythia` to the cross section times the luminosity $\sigma \times \mathcal{L}$ (which corresponds to the line "Initial number of events"), we applied a Missing Transverse Energy (MET) filter $E_T^{\mathrm{miss}} > 80$ GeV at the Monte-Carlo level. The number of events after this filter corresponds to the "ALL" number in Fig. 47 of [3]. This explains why for the benchmark $(m_{\tilde{t}_1}, m_{\tilde{\chi}_1^0}) = (200, 125)$ and $(m_{\tilde{t}_1}, m_{\tilde{\chi}_1^0}) = (200, 195)$ GeV the "ALL" numbers differ, although we have equal stop masses. This number then corresponds to the line "$E_T^{\mathrm{miss}} > 80$ GeV Filter" in Tables 1, 2, 3.

The next cut applied is a MET preselection at the reconstructed level of $E_T^{\mathrm{miss}} > 100$ GeV. At this threshold, the ATLAS MET trigger is not fully efficient. To reproduce the MET trigger efficiency we parametrised the efficiency turn-on curve presented in [9] coming from the ATLAS simulation of the process $pp \to ZH \to \nu\bar{\nu}b\bar{b}$, as advised after communication with the ATLAS SUSY conveners. We already observe at this level a discrepancy which ranges from 16% to 32%

for the three benchmark points when comparing our implementation to the ATLAS results. Moreover we cannot reproduce the trigger, event Cleaning, and bad jet veto efficiencies, as we do not have official access to this information. We leave a blank in our results, and only quote the ATLAS number after the bad bet veto requirement. Among these three requirements, the ATLAS trigger efficiency leads to the major contribution.

We next only quote the surviving number of events after the electron and muon vetoes ("Lepton veto") since in principle the simulated signal sample should not contain primary leptons. The relative change quoted at this line c, is calculated with respect to the line $E_T^{\text{miss}} > 100$ GeV.

After the lepton veto, the relative efficiencies of the remaining preselection cuts are quite similar between our reimplementation and the official ATLAS results. The largest discrepancy observed concerns the leading jet p_T cut $p_T > 150$ GeV for the benchmark $(m_{\tilde{t}_1}, m_{\tilde{\chi}_1^0}) = (200, 125)$ GeV and reaches $\sim 8\%$. This discrepancy can partly be due to our mismatch in the MET efficiencies which should impact the leading jet transverse momentum. Although at the level of the MET cut $E_T^{\text{miss}} > 150$ GeV, the MET trigger efficiency is 100%, we still get some discrepancies when absolute numbers are compared. Such a discrepancy is caused by a mismatch in the $E_T^{\text{miss}} > 100$ GeV and trigger efficiencies which impacts all preselection cuts in-between.

Once the signal regions are concerned, the relative efficiencies of our cuts with respect to the official ones are comparable, although the E_T^{miss} cuts still exhibits the largest differences.

2.2   Histograms

Let us now turn our attention to the comparison with some of the existing official histograms which are displayed in Fig. 1. There are four of them: the pseudo-rapidity η of the leading jet (top, left), the preselected missing energy distribution (top, right), the jet multiplicity (bottom,left) and the $\Delta\phi(E_T^{\text{miss}}, \text{jets})$ distribution (bottom,right). Only the distributions for the $(m_{\tilde{t}_1}, m_{\tilde{\chi}_1^0}) = (200, 125)$ and $(m_{\tilde{t}_1}, m_{\tilde{\chi}_1^0}) = (200, 195)$ are available on the Twiki page of the analysis [3]. Overall the agreement is quite good. The largest discrepancy is observed in the the preselected E_T^{miss}, figure (top, right), for the benchmark $(m_{\tilde{t}_1}, m_{\tilde{\chi}_1^0}) = (200, 125)$.

2.3   Exclusion plot

We also produced the 95% exclusion contour derived from the monojet recasted analysis, targeting $\tilde{t}_1 \to c + \tilde{\chi}_1^0$ with 100% branching fraction. For the statistical interpretation, we make use of the module `exclusion_CLs.py` provided in the `MadAnalysis5` recasting tools. Given the number of signal, expected and observed background events, together with the background uncertainty (both directly taken from the experimental publications), `exclusion_CLs.py` determines the most sensitive signal region (SR), the exclusion confidence level using the CL_s prescription from the most sensitive SR, and the nominal cross section σ_{95} that is excluded at 95% CL. The results can be found in Fig. 2.

The 95% CL exclusion contour obtained from the recasted `MA5` monojet analysis lies between the ATLAS $\pm 1\sigma$ theoretical uncertainty 95% CL exclusion contours. The issue in the E_T^{miss} description raised from the cutflows seem to have little impact on the limits.

cut	$\tilde{t} \to c\tilde{\chi}_1^0$ (200/125) cutflow			
	# events (scaled to σ and $\mathcal{L}$)	relative change	# events (official)	relative change (official)
Initial number of events	376047.3	376047.3		
$E_T^{\mathrm{miss}} > 80$ GeV Filter	192812.8	-48.7%	181902.0	181902.0
$E_T^{\mathrm{miss}} > 100$ GeV	136257.1	-29.3%	97217.0	-46.6%
Trigger, Event cleaning...	-	-	82131.0	
Lepton veto	134894.2	-1.0%	81855.0	-15.8%
$N_{\mathrm{jets}} \leq 3$	101653.7	-24.6%	59315.0	-27.5%
$\Delta\phi(E_T^{\mathrm{miss}}, \mathrm{jets}) > 0.4$	95568.8	-2.1%	54295.0	-8.5%
Leading jet $p_T > 150$ GeV	17282.8	-81.9%	14220.0	-73.8%
$E_T^{\mathrm{miss}} > 150$ GeV	10987.8	-36.4%	9468.0	-33.4%
M1 Signal Region				
Leading jet $p_T > 280$ GeV	2031.2	-81.5%	1627.0	-82.8%
$E_T^{\mathrm{miss}} > 220$ GeV	1517.6	-25.3%	1276.0	-21.6%
M2 Signal Region				
Leading jet $p_T > 340$ GeV	858.0	-92.2%	721.0	-92.4%
$E_T^{\mathrm{miss}} > 340$ GeV	344.4	-59.9%	282.0	-60.9%
M3 Signal Region				
Leading jet $p_T > 450$ GeV	204.3	-98.1%	169.0	-98.2%
$E_T^{\mathrm{miss}} > 450$ GeV	61.3	-70.0%	64.0	-62.1%

Table 1: Cutflow for the benchmark point $\tilde{t} \to c\tilde{\chi}_1^0$ (200/125) in the three Signal Regions.

	$\tilde{t} \to c\tilde{\chi}_1^0$ (200/195) cutflow				
cut	# events (scaled to σ and $\mathcal{L}$)		relative change	# events (official)	relative change (official)
Initial number of events	376047.3		376047.3		
$E_T^{\mathrm{miss}} > 80$ GeV Filter	104577.6		-72.2%	103191.0	103191.0
$E_T^{\mathrm{miss}} > 100$ GeV	82619.0		-21.0%	64652.0	-37.3%
Trigger, Event cleaning...	-		-	57566.0	
Lepton veto	82493.9		-0.2%	57455.0	-11.1%
$N_{\mathrm{jets}} \leq 3$	75391.5		-8.6%	52491.0	-8.6%
$\Delta\phi(E_T^{\mathrm{miss}}, \mathrm{jets}) > 0.4$	70888.1		-1.2%	49216.0	-6.2%
Leading jet $p_T > 150$ GeV	25552.0		-64.0%	20910.0	-57.5%
$E_T^{\mathrm{miss}} > 150$ GeV	21569.1		-15.6%	18297.0	-12.5%
M1 Signal Region					
Leading jet $p_T > 280$ GeV	4922.0		-77.2%	3854.0	-78.9%
$E_T^{\mathrm{miss}} > 220$ GeV	4628.4		-6.0%	3722.0	-3.4%
M2 Signal Region					
Leading jet $p_T > 340$ GeV	2509.0		-88.4%	1897.0	-89.6%
$E_T^{\mathrm{miss}} > 340$ GeV	1758.9		-29.9%	1518.0	-20.0%
M3 Signal Region					
Leading jet $p_T > 450$ GeV	773.3		-96.4%	527.0	-97.1%
$E_T^{\mathrm{miss}} > 450$ GeV	476.8		-38.3%	415.0	-21.3%

Table 2: Cutflow for the benchmark point $\tilde{t} \to c\tilde{\chi}_1^0$ (200/195) in the three Signal Regions.

cut	$\tilde{t} \to c\tilde{\chi}_1^0$ (250/245) cutflow			
	# events (scaled to σ and $\mathcal{L}$)	relative change	# events (official)	relative change (official)
Initial number of events	113192.0	113192.0		
$E_T^{\mathrm{miss}} > 80$ GeV Filter	36055.4	-68.1%	48103.0	48103.0
$E_T^{\mathrm{miss}} > 100$ GeV	29096.3	-19.3%	23416.0	-51.3%
Trigger, Event cleaning...	-	-	21023.0	
Lepton veto	29041.8	-0.2%	20986.0	-10.4%
$N_{\mathrm{jets}} \leq 3$	26295.2	-9.5%	18985.0	-9.5%
$\Delta\phi(E_T^{\mathrm{miss}}, \mathrm{jets}) > 0.4$	24676.9	-1.4%	17843.0	-6.0%
Leading jet $p_T > 150$ GeV	9652.1	-60.9%	8183.0	-54.1%
$E_T^{\mathrm{miss}} > 150$ GeV	8363.0	-13.4%	7290.0	-10.9%
M1 Signal Region				
Leading jet $p_T > 280$ GeV	2156.1	-74.2%	1748.0	-76.0%
$E_T^{\mathrm{miss}} > 220$ GeV	2022.9	-6.2%	1694.0	-3.1%
M2 Signal Region				
Leading jet $p_T > 340$ GeV	1107.4	-86.8%	882.0	-87.9%
$E_T^{\mathrm{miss}} > 340$ GeV	817.5	-26.2%	736.0	-16.6%
M3 Signal Region				
Leading jet $p_T > 450$ GeV	376.1	-95.5%	279.0	-96.2%
$E_T^{\mathrm{miss}} > 450$ GeV	268.0	-28.7%	230.0	-17.6%

Table 3: Cutflow for the benchmark point $\tilde{t} \to c\tilde{\chi}_1^0$ (250/240) in the three Signal Regions.
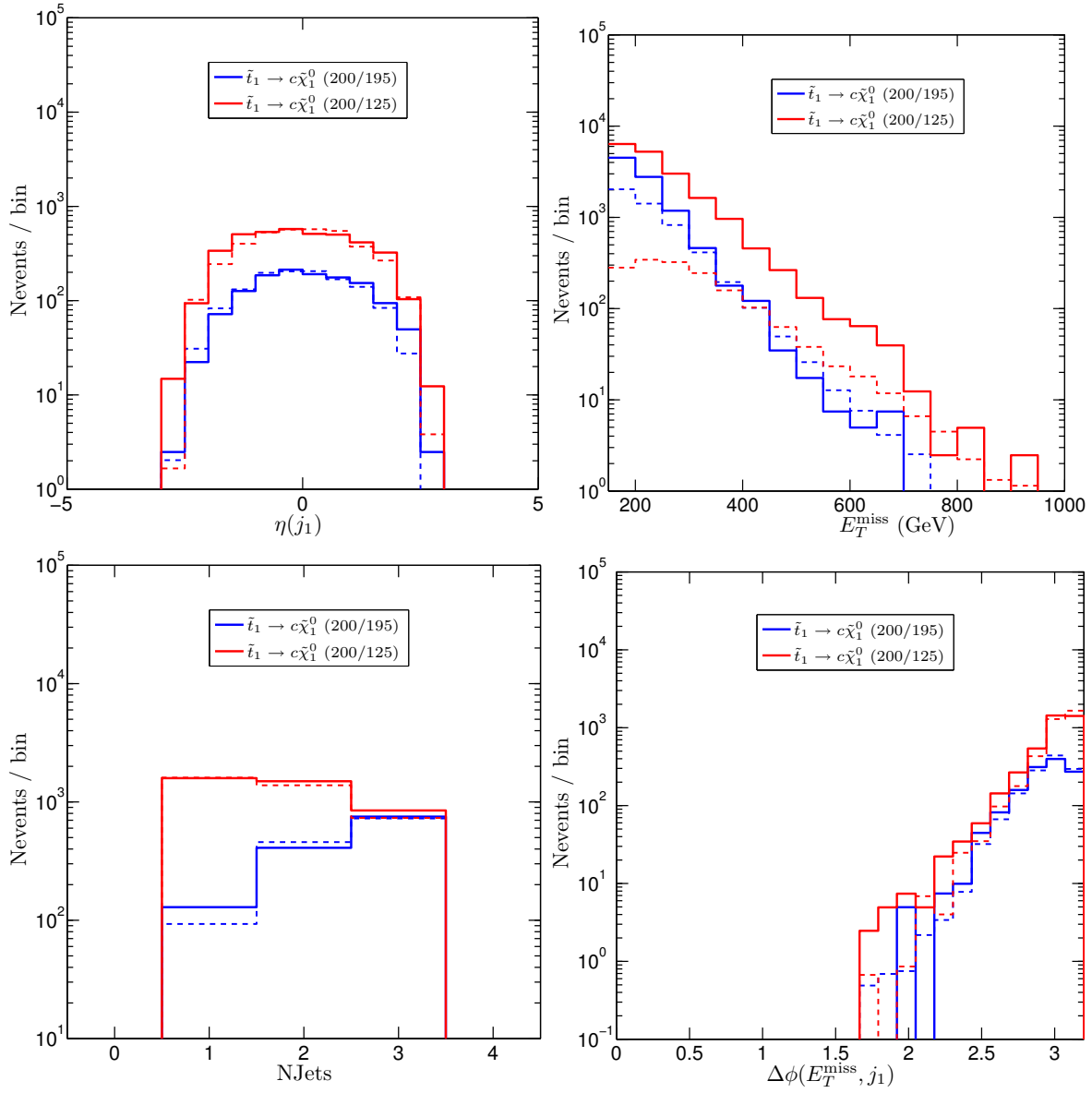
Figure 1: *Official results: dashed lines, MA5 results: solid lines*
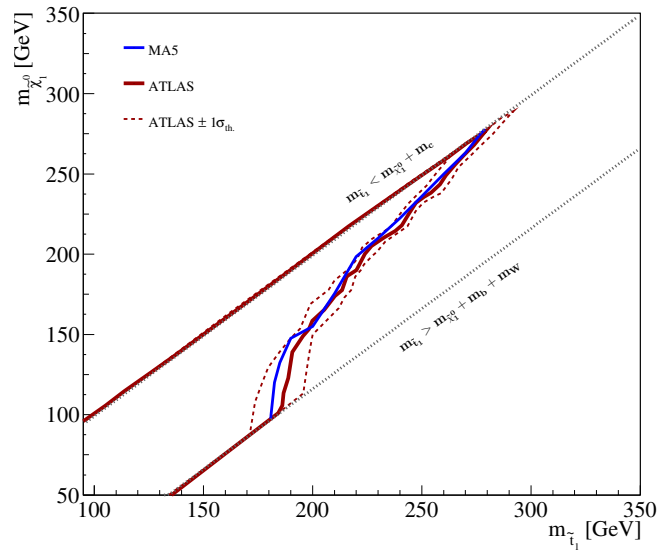
Figure 2: *95% CL exclusion contour of the monojet analysis targeting the decay $\tilde{t}_1 \to c + \tilde{\chi}_1^0$.* *The blue solid line corresponds to the* **MA5** *result, the red solid line the ATLAS result, and the dashed lines the ATLAS exclusion limits with a theoretical uncertainty of $\pm 1\sigma$.*

References

[1] G. Aad et al. (ATLAS), Phys.Rev. **D90**, 052008 (2014), `1407.0608`.

[2] E. Conte, B. Fuks, and G. Serret, Comput.Phys.Commun. **184**, 222 (2013), `1206.1599`.

[3] `https://atlas.web.cern.ch/Atlas/GROUPS/PHYSICS/PAPERS/SUSY-2013-21`.

[4] J. Alwall, M. Herquet, F. Maltoni, O. Mattelaer, and T. Stelzer, JHEP **1106**, 128 (2011), `1106.0522`.

[5] `http://cds.cern.ch/record/1303025`.

[6] `http://hepdata.cedar.ac.uk/view/ins1304459`.

[7] J. de Favereau, C. Delaere, P. Demin, A. Giammanco, V. Lemaître, et al. (2013), `1307.6346`.

[8] `http://madanalysis.irmp.ucl.ac.be/wiki/PhysicsAnalysisDatabase`.

[9] `https://twiki.cern.ch/twiki/bin/view/LHCPhysics/SUSYCrossSections8TeVstopsbottom`.

[9] `https://twiki.cern.ch/twiki/bin/view/AtlasPublic/MissingEtTriggerPublicResults`.